Advances in Nano Research, *Vol. 13, No.5 (2022) 499-512*
https://doi.org/10.12989/anr.2022.13.5.499

Estimation of lightweight aggregate concrete characteristics using a novel stacking ensemble approach

Mosbeh R. Kaloop[1,2,3a], Abidhan Bardhan[4b], Jong Wan Hu[*1,2] and Mohamed Abd-Elrahman[5c]

[1]*Department of Civil and Environmental Engineering, Incheon National University, Incheon, Korea*
[2]*Incheon Disaster Prevention Research Center, Incheon National University, Incheon, Korea*
[3]*Public Works Engineering Department, Mansoura University, Mansoura, Egypt*
[4]*Department of Civil Engineering, National Institute of Technology Patna, India*
[5]*Structural Engineering Department, Mansoura University, Mansoura, Egypt*

(*Received February 9, 2022, Revised September 25, 2022, Accepted September 26, 2022*)

Abstract. This study investigates the efficiency of ensemble machine learning for predicting the lightweight-aggregate concrete (LWC) characteristics. A stacking ensemble (STEN) approach was proposed to estimate the dry density (DD) and 28 days compressive strength (Fc-28) of LWC using two meta-models called random forest regressor (RFR) and extra tree regressor (ETR), and two novel ensemble models called STEN-RFR and STEN-ETR, were constructed. Four standalone machine learning models including artificial neural network, gradient boosting regression, K neighbor regression, and support vector regression were used to compare the performance of the proposed models. For this purpose, a sum of 140 LWC mixtures with 21 influencing parameters for producing LWC with a density less than 1000 kg/m^3, were used. Based on the experimental results with multiple performance criteria, it can be concluded that the proposed STEN-ETR model can be used to estimate the DD and Fc-28 of LWC. Moreover, the STEN-ETR approach was found to be a significant technique in prediction DD and Fc-28 of LWC with minimal prediction error. In the validation phase, the accuracy of the proposed STEN-ETR model in predicting DD and Fc-28 was found to be 96.79% and 81.50%, respectively. In addition, the significance of cement, water-cement ratio, silica fume, and aggregate with expanded glass variables is efficient in modeling DD and Fc-28 of LWC.
Keywords: compressive strength; dry density; extra tree regressor; lightweight concrete; prediction; stacking ensemble

1. Introduction

One of the main disadvantages of conventional concrete is its high density compared to other construction materials which leading to increase the dead load of the structure members as well as increasing the overall cost of the buildings. It is responsible for more than 50% of the dead load of the building (Sikora *et al*. 2020). Lightweight concrete is considered an ideal solution for reducing the dead load of the structures, however, with reducing the density of the materials a significant decrease in strength is occurred (Sikora *et al*. 2020). It can be produced using different types of lightweight aggregates either natural or artificial (Chung *et al*. 2019). Mixture's composition and aggregates type are the main factors affecting the lightweight concrete characteristics. Structural performance of lightweight concrete can be assessed by determining the compressive strength, however, the dry density can be used as an indicator for physical performance of cement-based materials. To solve the problem of strength deterioration with decreasing the density of concrete, several researchers used nano-sized particles to improve the performance of lightweight concrete (Naniz and Mazloom 2018, Sikora *et al*. 2020, Abd-Elrahman *et al*. 2019, Narasimman *et al*. 2020, Du *et al*. 2015). With the addition of tiny-sized particle, the overall mechanical performance of concrete is significantly improved due microstructure densification and compactness as well as improvement of hydration process (Khater 2016, Shariati *et al*. 2020, Alsultan 2021, Tuhta 2021, Kasiri and Massah 2022).

The dry density (DD) and compressive strength at 28 days (Fc-28) are the primary characteristics that required for particular applications of LWC. Normally, destructive and non-destructive tests are used to estimate LWC characteristics (Hadianfard and Jafari 2016, Gouasmi *et al*. 2017, Fatahi and Jafari 2018, Kaloop *et al*. 2022). Destructive tests are not recommended for estimating the concrete characteristics of existing structures (Alwash 2017), and non-destructive tests have many errors in estimating concrete strength (Abd and Abd 2017). Therefore, the rabid and reliable prediction approaches that used machine learning, such as artificial neural network (ANN), support vector regression (SVR), regression, and genetic algorithms, have been developed for estimating LWC characteristics (Tavakkol *et al*. 2013, Hadianfard and Jafari 2016, Abd and Abd 2017). ANN was found an efficient technique to predict the strength of LWC compared to regression technique (Tavakkol *et al*. 2013, Yoon *et al*. 2019, Nagarajan *et al*. 2020), as well as that used in estimating other concrete properties (Kaloop *et al*. 2020, Lin and Wu 2021, Wu 2021). SVR provided a high

*Corresponding author, Professor,
E-mail: jongp24@inu.ac.kr
[a] Professor, E-mail: mosbeh@mans.edu.eg
[b] Ph.D. Student, E-mail: abidhan@nitp.ac.in
[c] Associate Professor, E-Mail: mohamedattia@mans.edu.eg

ISSN: 2287-237X (Print), 2287-2388 (Online)

Table 1 Descriptive statistics of variable used

Variable			ID	Unit	Category	Statistics				Significance	
						Mean	Max.	Min.	RSD	DD	Fc-28
Aggregate type	Expanded glass grading	0-1 mm	In-1	Kg/m^3	Input	82.22	332.00	0.00	91.38	√	√
		1-2 mm	In-2	Kg/m^3	Input	48.00	142.00	0.00	75.56	√	√
		2-4 mm	In-3	Kg/m^3	Input	53.67	186.00	0.00	86.67	√	√
	Expanded clay grading	0 -2 mm	In-4	Kg/m^3	Input	18.95	267.90	0.00	232.67	√	×
		1 - 4mm	In-5	Kg/m^3	Input	22.98	171.00	0.00	213.50	√	×
		2-8 mm	In-6	Kg/m^3	Input	40.76	310.00	0.00	186.99	√	√
	Ecoglass		In-7	Kg/m^3	Input	3.52	314.30	0.00	864.87	√	√
	Cement		In-8	Kg/m^3	Input	377.88	604.00	180.00	26.84	√	√
	Silica fume		In-9	Kg/m^3	Input	28.52	76.00	0.00	87.85	√	√
	Limestone powder		In-10	Kg/m^3	Input	2.24	155.00	0.00	731.02	√	√
	Fine fly ash		In-11	Kg/m^3	Input	1.00	140.00	0.00	1183.22	√	√
	Fly ash		In-12	Kg/m^3	Input	0.94	131.00	0.00	1183.22	√	√
	Quartz sand		In-13	Kg/m^3	Input	13.86	330.00	0.00	401.23	√	×
	Slag		In-14	Kg/m^3	Input	16.29	285.00	0.00	407.66	√	×
	Sand		In-15	Kg/m^3	Input	29.86	260.00	0.00	242.89	√	×
	Nanosilica		In-16	Kg/m^3	Input	3.04	48.00	0.00	308.82	√	√
	Short fiber		In-17	Kg/m^3	Input	0.23	9.10	0.00	488.77	√	√
	Long fiber		In-18	Kg/m^3	Input	0.44	10.80	0.00	373.12	√	√
	Superplasticizer		In-19	Kg/m^3	Input	4.82	22.40	0.00	64.51	√	√
	Stabilizer		In-20	Kg/m^3	Input	0.44	1.32	0.00	85.51	√	√
	water		In-21	Kg/m^3	Input	196.91	264.00	110.00	16.71	√	√
	Dry Density		DD	Kg/m^3	Output	770.35	1240.00	429.00	24.82		
	Fc-28		Fc-28	MPa	Output	13.04	32.00	3.04	46.94		

correlation with measured strength of lightweight foamed concrete (Abd and Abd 2017). However, a few studies using hybrid and more advantages machine learning techniques were used to estimate Fc of LWC. Moreover, DD of LWC did not predict through machine learning techniques yet according to authors best knowledge.

Recently, many researchers used boosting regression methods in predicting concrete characteristics. For instance, Nguyen-Sy *et al*. (2020) applied extreme gradient boosting regression (XGB) in predicting uniaxial compressive strength of concrete and compared it to ANN and SVR, the results demonstrated the XGB is more powerful than other machine learning techniques in predicting concrete strength. In addition, XGB was compared to conventional and hybrid ANN, and the results provided the accuracy of it is efficient in compressive strength of concrete (Cui *et al*. 2021). The GBR obtained the highest accuracy in predicting compressive strength of incorporating phase change materials into cementitious composites compared to random forest regressor (RFR), extra tree regressor (ETR), and XGB methods (Marani and Nehdi, 2020). Other significant results for using boosting regression methods can be found in (Anyaoha *et al*. 2019, Koya *et al*. 2021, Wan *et al*. 2021, Wong *et al*. 2021). Meanwhile, the performance of KNR was shown high for predicting the compressive strength of high performance concrete (Abubakar and Tabra 2019). In addition, a comparative study for predicting blast ground vibration showed that the hybrid KNR is more significant than SVR and RFR (Bui *et al*. 2019). The KNR was used to estimate the geopolymerization process of fly ash-based geopolymer, and the results showed that the accuracy of KNR was 91.62%, 88.36%, 92.86 and 90.60% for predicting the geopolymerization peak time and peak heat and dissolution peak time and peak heat, respectively (Tanyildizi 2021). More recently, hybrid ensemble models have been development in prediction applications for concrete properties and others engineering applications (Asteris *et al*. 2021, Chakraborty *et al*. 2021, Zhou *et al*. 2021). The stacking ensemble (STEN) models are one of the hybrid techniques. STEN uses more than one soft computing techniques, and it feeds the outputs of base-learners into one combiner (Lee and Ahn 2021). Here, based on our literature, the STEN-RFR and STEN-ETR have not been used for estimating the concrete characteristics.

This study aims to develop advanced machine leaning techniques for modeling DD and Fc-28 of LWC. ANN, SVR, gradient boosting regression (GBR), K neighbor regression (KNR) are evaluated and compared in this study. Integrated SVR, GBR and KNR with random forest

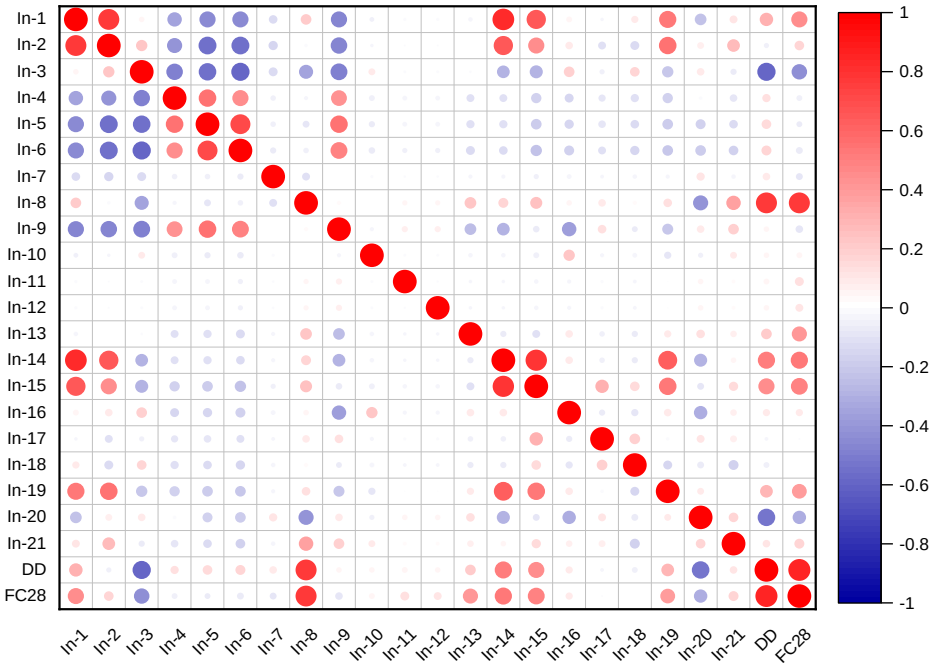

Fig. 1 Pearson correlation matrix

regressor (RFR) and extra tree regressor (ETR), simply there are stacking ensemble model with RFR (STEN-RFR) and stacking ensemble model with ETR (STEN-ETR), respectively, are designed and evaluated as new hybrid techniques. Therefore, the contributions of this study are: (1) In using novel hybrid ensemble models, STEN-RFR and STEN-ETR, to model the DD and Fc-28 of the LWC, (2) In evaluating GBR and KNR for modeling the LWC properties, (3) In developing new machine learning approaches for modeling DD of LWC, and (4) In studying the impact of components materials that used for producing LWC with density less than 1000 kg/m3 in predicting DD of Fc-28. For that, data of 140 LWC mixtures were prepared and used in this study to design and evaluate the proposed models.

2. Data used and description

To simulate a wide range of LWC results, experimental datasets were designed and collected. Table 1 presents the input and output variables that used in this study and those statistical parameters, including mean, maximum (Max), minimum (Min), and relative standard deviation (RSD). 21 input variables were used in this study to produce LWC with density lower than 1000 Kg/m^3 and estimate that DD and Fc-28 characteristics. Lightweight aggregate with different expanded glass and expanded clay gradations and Eco-glass (foamed glass) were used. From Table 1, it can be seen that the range of input variables is high, for instance the range of cement content is in between 180 and 604 Kg/m^3, and water content range is 110 to 264 Kg/m^3. This gives a high possibility to use the proposed models in that modeling the LWC properties. The means and RSD show the distortion of input variables is high, i.e., reach up to 1183.22%. This means that the relationship between inputs and outputs variables is nonlinear and complex. For more understanding this relationship, the ANOVA technique was used to measure the linear significant between inputs and outputs variables, as presented in Table 1. In addition, Figs 1 and 2 demonstrate the correlation matrix (based on Pearson correlation coefficient) and frequency histogram, respectively, of the collected dataset. From Table 1 it can be observed that all variables have significant impact in modeling DD, while 16 variables impact the Fc-28 of LWC. This means that the linearity relationship between DD and input variables is higher than that for Fc-28, and this gives the possibility of using all variables in modeling DD. In addition, the correlation between inputs and outputs shows that both have the same trend of correlation with input variables. In general, the correlation between inputs and DD variables is higher than between inputs and Fc-28. However, variables In-1, In-3, In-8, In-14, In-15, In-19, and In-20 have a high linear correlation with DD and Fc-28. Here, a conflict statistical evaluation can be detected from these results. This indicates that the presented statistical evaluation may not be suitable for evaluating the sensitivity of input variables in modeling DD and Fc-28 of LWC. Thus, accurate relationship between input and output variables cannot be linearly detected, since the rate change of input variables is not significant. For that, the sensitivity of input variables in modeling DD and Fc-28 are evaluated and discussed in the current work.

3. Theory and proposed models

3.1 Artificial neural network

The feedforward ANN is well known in the literature, and it is used in this paper. Basically, ANN comprises three layers, input, hidden and output, as presented in Fig. 3.

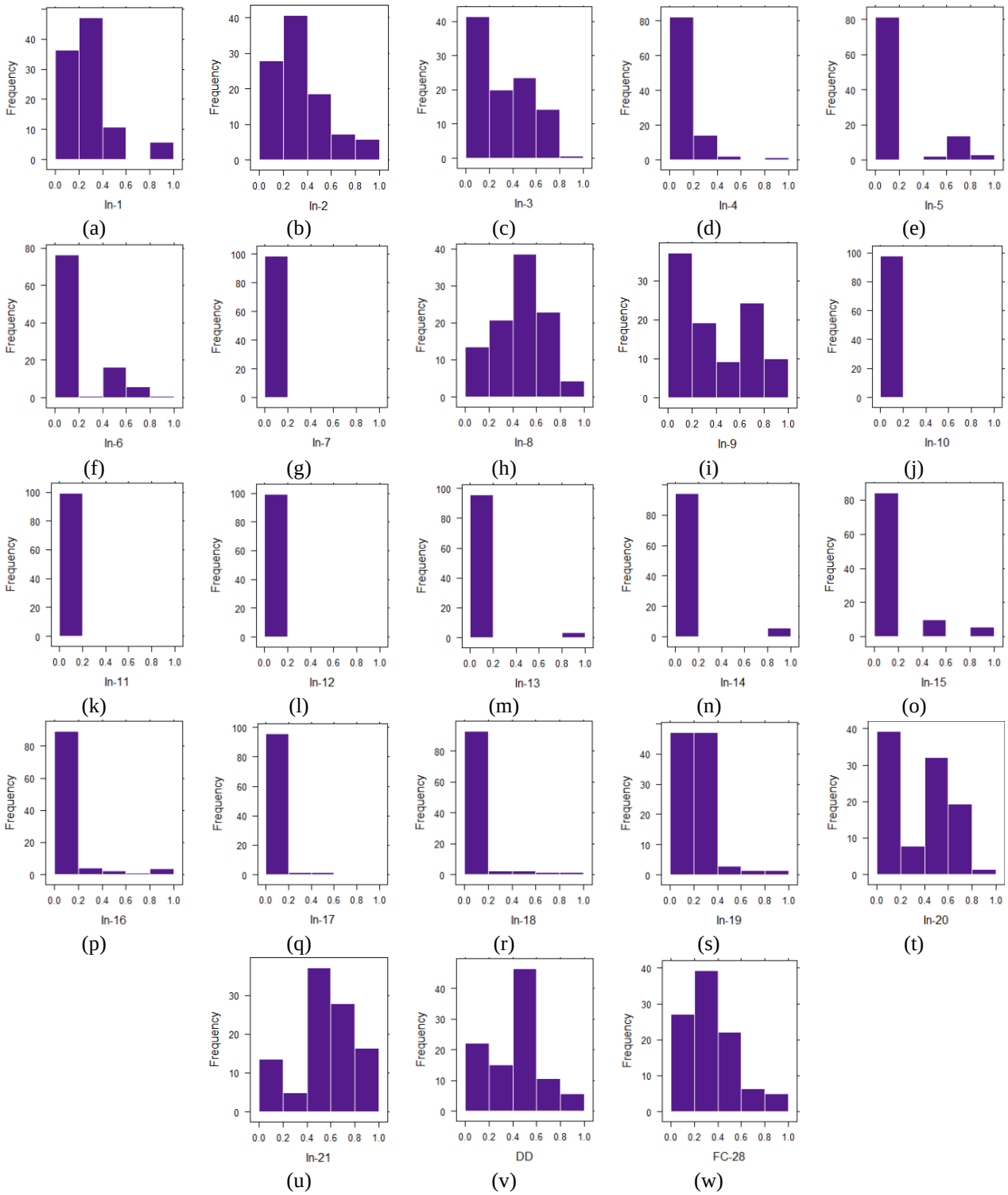

Fig. 2 Frequency histogram of input and output variables

Twenty-one input neurons and two output neurons are used in the current study. The trail-and-error through tunning process based on estimating low model error term in mean square error is applied to estimate the number of hidden layers and that neurons. The main theory and structures of ANN can be found in (Braspenning *et al*. 1995, Abdelaziz *et al*. 2020, Meshram *et al*. 2020, Sedghi *et al*. 2021). The neuron output can be expressed as follows:

$$O_j = f(\sum_i w_{ij} x_{ij}) \quad (1)$$

where O_j represents the output of neuron j, f denotes the transfer function, w_{ij} are the weight connection between neurons i and j. x_{ij} are the inputs from nodes i to nodes j. As presented in Eq. (1), the main parameter is the weight. The trail-and-error method is used to estimate the weight variable.

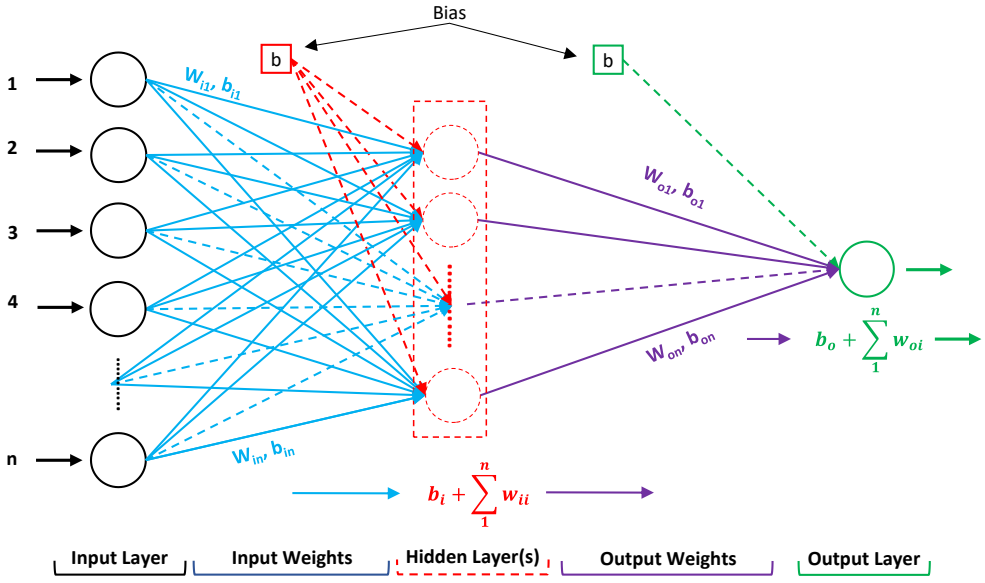

Fig. 3 A basic structure of ANN with single hidden layer

3.2 Details of base models

The proposed stacking-based ensemble model necessitates the use of multiple base-learners in order to accurately predict streamflow. Furthermore, as Alpaydin (2020) suggests, the base-learners should be informative and diverse, so that they complement one another. In this study, three different modelling techniques, including gradient boosting regressor (GBR), K-neighbor regression (KNR), and support vector regressor (SVR), were used as the base models. The sub-sections that follow provide a brief overview of these three standalone methods.

3.2.1 Gradient boosting regressor

The GBR is used for regression and classification algorithms based on an ensemble of decision tree (Nguyen-Sy *et al*. 2020, Lee and Ahn 2021, Wong *et al*. 2021). It implements for fitting the new predictor to the residual of errors that generated from the previous predictor under the gradient boosting framework (Wan *et al*. 2021). The mapping function $F(x)$ between random input variables (x) and response variable (y) can be estimated through minimizing loss function $L(y, F(x)$ (Nie *et al*. 2021). The seek function $(\tilde{F}(x))$ for reducing the prediction error can be estimated through:

$$\tilde{F}(x) = arg_{F(x)} min L_{y,x}(y, F(x)) \tag{2}$$

where the loss function can be estimated as a square error function $(L(y, F(x)) = (y - F(x))^2)$ (Nie *et al*. 2021). An initial base learner is assumed first as a constant function, and then a steepest descent step is applied for the minimization of the loss function. To find the local minimum of the loss function, steepest descent generates steps proportional to the negative gradient of it. The gradient loss function can be determined as follows:

$$\tilde{y}_i = -\left[\frac{\partial L(y_i, F(x_i))}{\partial (F(x_i))}\right]_{F(x)=F_{m-1}(x)}, i = 1,2,\dots,N \tag{3}$$

The regression trees h(xi,a), where a represents weak learner, are used to determine range of the gradient. The tree can be estimated as follows:

$$a_m = arg_{a,\beta} min \sum_{i=1}^{N} (\tilde{y}_i - \beta h(x_i, a))^2 \tag{4}$$

where a_m represents the parameters that obtained at iteration m, β denotes the weight of each weak learner. Each regression tree is fitted to the current negative gradient, subsequently, the optimal length (ρ_m) and the model $(F_m(x))$ can be determined and updated as follows (Friedman, 2001, Nie *et al*. 2021):

$$\rho_m = arg_\rho min \sum_{i=1}^{N} L(y_i - F_{m-1}(x_i) + \rho h(x_i, a)) \tag{5}$$

$$F_m(x) = F_{m-1}(x) + \rho_m h(x, a_m), \ \ m = 1,2,\dots,M \tag{6}$$

This algorithm can be used in classification and regression, in the current study, it uses for regression. Here, the trees or decision trees is the use of recursive methods to generate binary trees. For prediction concrete characteristic, here, the square error minimization criterion is applied to estimate the optimal regression trees.

3.2.2 K-neighbor regression

The KNN is a nonparametric regression estimator depends on local versions of local estimator (Altman 1992). During the training phase of the algorithm, k class centres are estimated. Then, in the testing phase, the data is classified based on the distance to the class centres. The Euclidean, Minkowski, and Manhattan distances can be used (Tanyildizi, 2021). In the current study, the Euclidean distance is used, and it can be expressed as follows:

$$d = \sqrt{\sum_{i=1}^{N} (x_{tes,i} - x_{tr,i})^2} \tag{7}$$

where x_{tes} and x_{tr} are the testing and training samples, and N is the data dimension. Here, the steps to obtained the best solution can be summarized as follows (Tanyildizi, 2021): a) the distance between qualitative values of testing to each training is determined, b) the results of d are sorted to the lowest and predetermined neighbors c) the calculation of the highest number refers to the estimation results, and d) the KNN determine the accuracy based on the estimation.

3.2.3 Support vector regressor

The SVR is the regression category of the support vector machine, and it was introduced by Vapnik (1995). SVR was used in modeling different properties of concrete structures (Pal and Deswal 2011, Chou *et al*. 2016). Pal and Deswal (2011) and Mozumder *et al*. (2017) proposed the SVR formulas and theory in nonlinear prediction of shear strength of beams. Vapnik (1995) proposed that in SVR, "a fixed mapping procedure to map its input to an n-dimensional feature space, then nonlinear functions are fit the high-dimensional the features". In hyperspace, the nonlinear function of SVR can be expressed as follows:

$$f(x) = w.\varphi(x) + b \tag{8}$$

where w and φ represent the weight vector and transformation functions, respectively, x is the input vector, and b denotes a scalar. In Eq. (8), the w and b are used to determine the normal vector and scalar, respectively, for the high-dimensional space, which determined through $\varphi(x)$. This function can be obtained using the "ε-insensitive" loss function. The loss function is used as a threshold to remove the model residuals that do not contribute the model accuracy. The solution of Eq. 8 depends on the training pattern of Lagrange multipliers ($\alpha_i^*$and α_i), which are only applied to estimate the w and b. Therefore, the kernel function is commonly used to solve the nonlinear regression problems in SVR. The Kernel functions can transform the nonlinear problems to linear problems, as presented in Yaseen *et al*. (Yaseen *et al*. 2018), which allows the SVR to solve more complex problems. Thus, the nonlinear SVR can be rewritten as follows:

$$f(x) = \sum_{nsv} (\alpha_i^* - \alpha_i) K(x_i.x) + b \tag{9}$$

where, nsv represent number of support vectors, K is the kernel function, $K(x_i.x) = (\varphi(x_i).\varphi(x))$. In the current study, the radial basis kernel (RBF) is applied.

3.3 Random forest regressor

RFR is the most commonly used algorithm due to its simplicity and ease of measuring the prediction factors (Sandhu and Batth, 2021). It is based on the idea of a collection of large corelated decision trees (DTs). In RFR, random forest (RF) creates multiple trees and then combines them at the end to produce accurate and stable results. The RFR method combines the decisions of individual trees and aids in improving accuracy. For randomness, it employs bootstrap aggregation for improving the accuracy and stability. The bootstrap aggregation can be mathematically expressed as:

$$bagging = \frac{1}{B}\sum_{b=1}^{B} f_b(\hat{x}) \tag{10}$$

where $\hat{x}$ is the predictions for unseen samples b is the number of tress i.e., b = 1.2.3, …. B, and f_b represents training of a DT model in a random forest model. More mathematical details of RFR working principle can be found in the literature of Sandhu and Batth (2021), Zanoni *et al*. (2015), and Sidiq *et al*. (2018).

3.4 Extra-tree regressor

Extra-trees and RF are two very similar ensemble methods with nearly identical working principles (Geurts *et al*. 2006). The main distinctions, however, are as follows: (a) RF employs bootstrap replicas, or subsamples the input data with replacement, whereas extra trees (ETs) employ the entire sample. There is an optional parameter in the ETs implementation that allows users to bootstrap replicas. This may increase variance because bootstrapping diversifies it, and (b) another difference is the choice of cut points to split nodes. RF selects the optimal split, whereas ETs select it at random. However, once the split points are chosen, the two algorithms select the best one from the subset of features. As a result, ETs introduces randomization while maintaining optimization. The ETR algorithm is faster in terms of computational cost. This algorithm saves time because the entire procedure is the same, but it chooses the split point at random rather than calculating the optimal one (Geurts *et al*. 2006).

3.5 Stacking ensemble modelling

As a group of experts, ensemble models are defined as meta-algorithms that combine many standalone machine learning models (known as weak learners) into a single predictive model. Researchers and the machine learning community have recently discovered a variety of advantages to using such an approach in automated decision-making applications, particularly in the engineering field. The efficiency of ensemble learners outperforms that of individuals. From a statistical standpoint, it is undeniable that acceptable regressor efficiency on the training dataset does not imply excellent efficiency on data not used during training. This means that even if the testing dataset is not a fair representation of potential field data, machine learning algorithms with similar generalisation efficiencies will have different predictive efficiencies. This is why combining the outputs of multiple learners can help reduce the likelihood of making an incorrect prediction.

Stacking ensemble machine learning algorithm is a technique that incorporates multiple prediction models into a single model and works at different levels or layers. This technique introduces the concept of meta-learning, which seeks to reduce generalisation errors by reducing the bias of its generalisers, resulting in an asymptotically optimal learning system. Assume a stacking ensemble machine learning algorithm that uses two levels/layers, level-0 and level-1 (as shown in Fig. 4). At level 0, several standalone

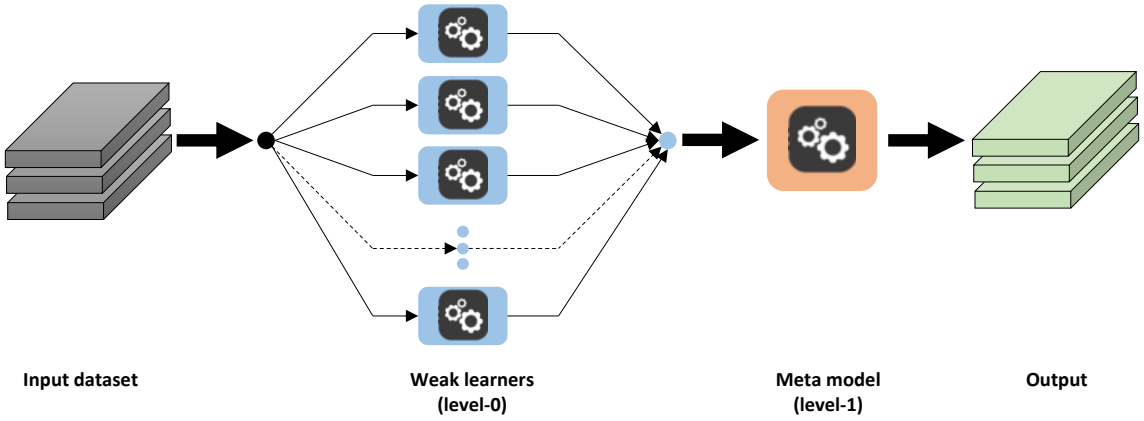

Fig. 4 Flow chart showing the working principle of stacking ensemble model

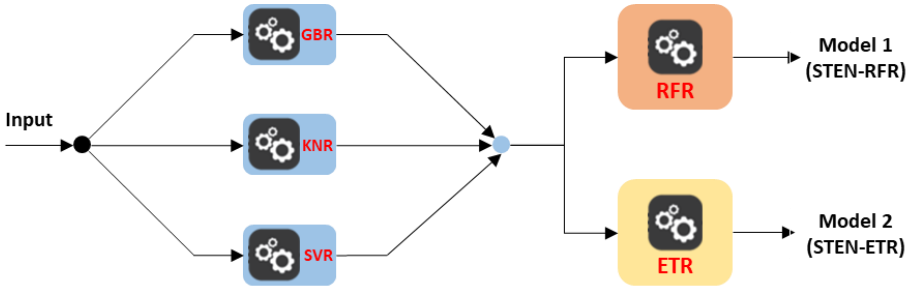

Fig. 5 Construction diagram of STEN-RFR and STEN-ETR models

models are trained, and the response variable for each is predicted. These predictions are used as an input set by the level-1 model. This model, dubbed a meta-model, is trained, and the predictions it generates are the expected outcomes. In general, the subsequent level model learns from the previous level models, with each level's model immediately providing its best estimations. In other words, the level-1 model learns from the predictions of the level-0 models. It should be emphasised that the number of levels does not have to be limited to two. The rule is that the n-1 level models' predictions should be used in the n-level model. When using a stacking ensemble machine learning algorithm, the key modification in the predictive results is when there is diversity between the models with different levels, because models with different generalisation principles produce different results. As a result, the modelling process may include diversity if models are used in conjunction with various learning strategies and data characteristics and observations.

Fig. 4 depicts a typical flow chart demonstrating the operation of the stacking ensemble model. As previously stated, the idea behind stacking is to learn multiple weak learners and combine them by training a meta-model to output predictions based on the multiple predictions returned by these weak models. As can be seen, the inputs are fed into level-0, which has one or more weak learners, which are then trained and the results are fed into level-1. In Level-1, there is a meta-model that combines the outputs of weak learners and generates a new output.

In this work, RFR and ETR were used as the meta-models to construct the proposed stacking ensemble models viz., STEN-RFR and STEN-ETR. For this purpose, three standalone models, namely GBR, KNR and SVR were used as the base models. The methodological development of STEN-RFR and STEN-ETR can be described as follows: (a) selection of input parameters, (b) selection of basic and hyper parameters of base models, (c) generation of training subset, (d) training the standalone models at level-0, (e) generation of level-0 outputs, (f) fed the level-0 outputs into level-1, i.e., output of GBR, KNR, and SVR models are fed into meta-models, and (g) construction of final models and generation of outputs. Fig. 5 displays the construction procedure of STEN-RFR and STEN-ETR models in predicting the DD and Fc-28 of LWC.

3.6 Performance assessments

To evaluate the accuracy of the proposed models, different statistical indices are used and evaluated. The Legate and McCabe`s Index (LMI), mean absolute error (MAE), Nash-Sutcliffe efficiency (NS), coefficient of correlation (R), root mean square error (RMSE), Root mean square error to observation`s standard deviation ratio (RSR), and variance account factor (VAF) were used to measure the model performance, The following equations present these indices calculation (Kaloop *et al.* 2020, Gabr *et al.* 2021):

$$LMI = 1 - \left[\frac{\sum_{i=1}^{n}|y_i - \hat{y}_i|}{\sum_{i=1}^{n}|y_i - y_{mean}|}\right] \quad (11)$$

$$MAE = \frac{1}{n}\sum_{i=1}^{n}|(\hat{y}_i - y_i)| \quad (12)$$

Table 2 Model performance in the training phase (for DD)

Indices	ANN	GBR	KNR	SVR	STEN-RFR	STEN-ETR
LMI	0.7846	0.6735	0.6130	0.8471	0.8138	0.8474
MAE	0.0400	0.0606	0.0718	0.0284	0.0345	0.0283
NS	0.9522	0.9081	0.8281	0.9637	0.9416	0.9669
R	0.9820	0.9785	0.9269	0.9825	0.9705	0.9834
RMSE	0.0529	0.0733	0.1003	0.0461	0.0584	0.0440
RSR	0.2187	0.3031	0.4147	0.1904	0.2416	0.1820
VAF	96.4259	90.8101	84.5108	96.4432	94.1750	96.6992

Table 3 Model performance in the testing phase (for DD)

Indices	ANN	GBR	KNR	SVR	STEN-RFR	STEN-ETR
LMI	0.5777	0.5208	0.5881	0.5758	0.7149	0.7725
MAE	0.0654	0.0743	0.0638	0.0657	0.0442	0.0352
NS	0.7483	0.8172	0.8152	0.7754	0.9270	0.9327
R	0.8966	0.9381	0.9072	0.8888	0.9645	0.9679
RMSE	0.1018	0.0868	0.0872	0.0962	0.0548	0.0527
RSR	0.5017	0.4275	0.4299	0.4740	0.2701	0.2595
VAF	75.0603	81.7349	81.5678	77.5361	92.8998	93.6040

$$NS = 1 - \frac{\sum_{i=1}^{n}(y_i - \hat{y}_i)^2}{\sum_{i=1}^{n}(y_i - y_{mean})^2} \quad (13)$$

$$R = \sqrt{\frac{\sum_{i=1}^{n}(y_i - y_{mean})^2 - \sum_{i=1}^{n}(y_i - \hat{y}_i)^2}{\sum_{i=1}^{n}(y_i - y_{mean})^2}} \quad (14)$$

$$RMSE = \sqrt{\frac{1}{n}\sum_{i=1}^{n}(y_i - \hat{y}_i)^2} \quad (15)$$

$$RSR = \frac{RMSE}{\sqrt{\frac{1}{n}\sum_{i=1}^{n}(y_i - y_{mean})^2}} \quad (16)$$

$$VAF\ (\%) = (1 - \frac{var(y_i - \hat{y}_i)}{var(y_i)}) \times 100 \quad (17)$$

where, $\hat{y}_i$ and y_i are the predicted and measured values, respectively, y_{mean} is the average of measured value, n is the data numbers, $var(y_i - \hat{y}_i)$ is the variance between predicted and measured values. For more investigation, visual statistical methods are used. The rank analysis, boxplot, and Taylor diagram are used to visualize the accuracy of the proposed models (Jalal *et al*. 2021, Kaloop *et al*. 2021, Khan *et al*. 2021).

4. Results and discussion

4.1 Model performance

Tables 2 and 3 and Fig. 6 present the statistical evaluation of the proposed models in the training and testing stages for predicting DD of LWC. The performance of the proposed model is high in the training stage with correlation between measured and predicted values reach to 0.98 for the ANN, SVR, and STEN.ETR models. The model error in terms RMSE is in between 0.04 Kg/m3 and 0.10 Kg/m3. The overall statistical indices show that STEN.ETR outperforms other models in the training stage with low MAE, RMSE, and RSR and high correlation in terms LMI, NS and R. In the testing stage, the hybrid models outperform other machine learning models. The model error of STEN.RFR and STEN.ETR is extremely low compared to other models. The RSR is 0.27 and 0.26 for STEN.RFR and STEN.ETR, respectively. The accuracy of both models in terms RMSE is 0.58 Kg/m3 and 0.44 Kg/m3, respectively. The VAF is a higher in the training and testing stages for the STEN.ETR model compared to other models. The overall statistical indices in the models' errors and correlation with measured DD show the STEN.ETR can be accurately used in modelling DD of LWC. In addition, from Fig. 6, a high correlation can be seen with low deviation (±10%) compared to experimental values for the STEN.ETR in modelling the DD in the training and testing phases. In addition, a low distortion around best fitting can be observed in the modelling DD of LWC using STEN.ETR model in the training and testing stages. Therefore, STEN.ETR provides an acceptable accuracy that can be consider it is as a robust soft computing technique can be used in estimating DD of LWC.

Meanwhile, the same proposed models through the same input variables are used to estimate the Fc-28 of LWC. Tables 4 and 5 and Fig. 6 show the statistical evaluations of the proposed models in modeling the Fc-28. In the training stage, the performance of the proposed models is high with high correlation between measured and predicted values approach more than 0.95 through SVR and STEN.ETR

Table 4 Model performance in the training phase (for FC-28)

Indices	ANN	GBR	KNR	SVR	STEN-RFR	STEN-ETR
LMI	0.5422	0.7109	0.4421	0.7779	0.7120	0.7389
MAE	0.0728	0.0460	0.0887	0.0353	0.0458	0.0415
NS	0.8402	0.8804	0.6504	0.9092	0.8860	0.9301
R	0.9418	0.9415	0.8488	0.9537	0.9417	0.9773
RMSE	0.0836	0.0723	0.1236	0.0630	0.0706	0.0553
RSR	0.3998	0.3458	0.5913	0.3013	0.3376	0.2643
VAF	88.4845	88.3442	66.9662	90.9505	88.6692	93.0149

Table 5 Model performance in the testing phase (for FC-28)

Indices	ANN	GBR	KNR	SVR	STEN-RFR	STEN-ETR
LMI	0.2980	0.2406	0.1940	0.3688	0.2763	0.4134
MAE	0.1105	0.1196	0.1269	0.0994	0.1140	0.0924
NS	0.5803	0.3638	0.3953	0.6053	0.5569	0.6568
R	0.7686	0.6341	0.6640	0.7836	0.7542	0.8150
RMSE	0.1392	0.1714	0.1671	0.1350	0.1431	0.1259
RSR	0.6478	0.7976	0.7776	0.6283	0.6657	0.5858
VAF	58.0767	38.0075	41.3229	61.3866	56.8490	66.1099

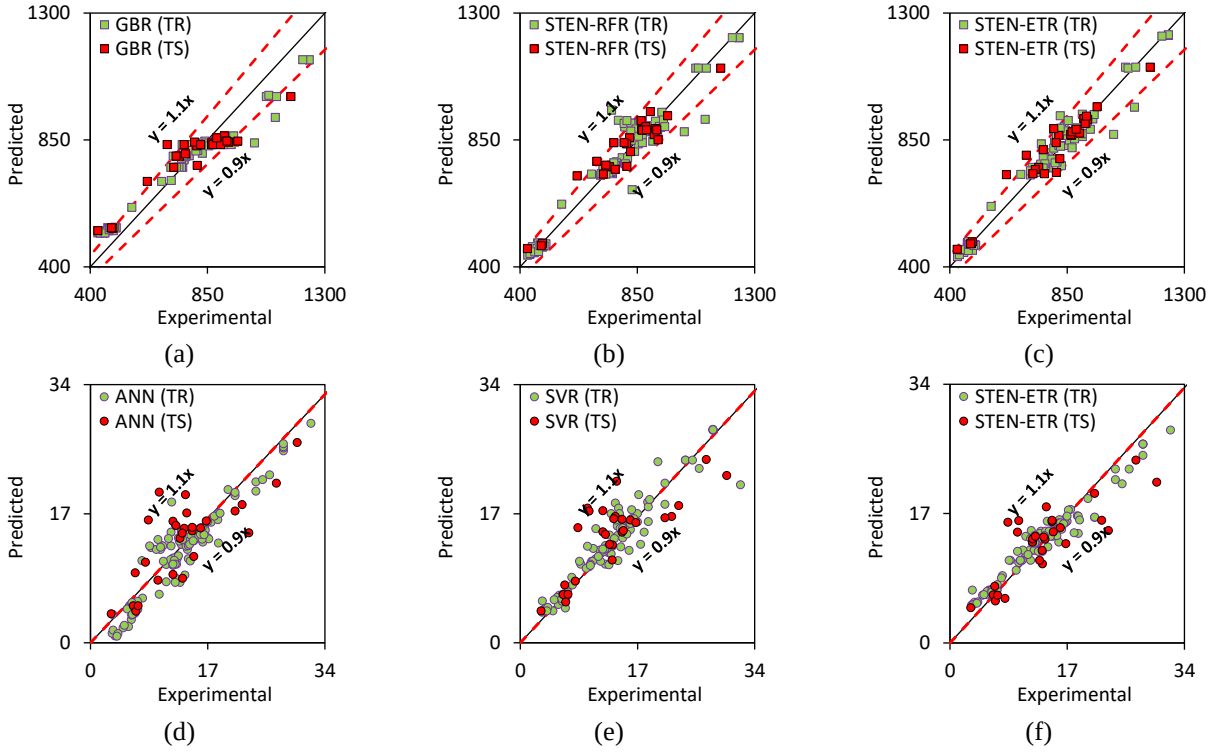

Fig. 6 Scatter plots for best three models (based on R2 value of testing phase) in training (TR) and testing phases (TS): (a-c) for DD prediction and (d-f) for FC-28 prediction

model. In addition, the overall statistical indices show the performance of STEN.ETR model is more accurate with correlation 0.98 and model accuracy 0.06 MPa in terms RMSE. However, the performance of all models is decreased in the testing stage. The high correlation (0.81) between measured and predicted Fc-28 is observed with using STEN.ETR model. The low model error indices, MAE, RMSE, and RSR, is observed with using STEN.ETR model. Also, high correlation indices, LMI, NS, and R, is observed for the STEN.ETR in the training and testing stages. VAF values are a higher for the STEN.ETR model compared to other proposed models. The overall statistical indices implies that the performance of STEN.ETR model is more acceptable to use in modeling Fc-28 of LWC. The

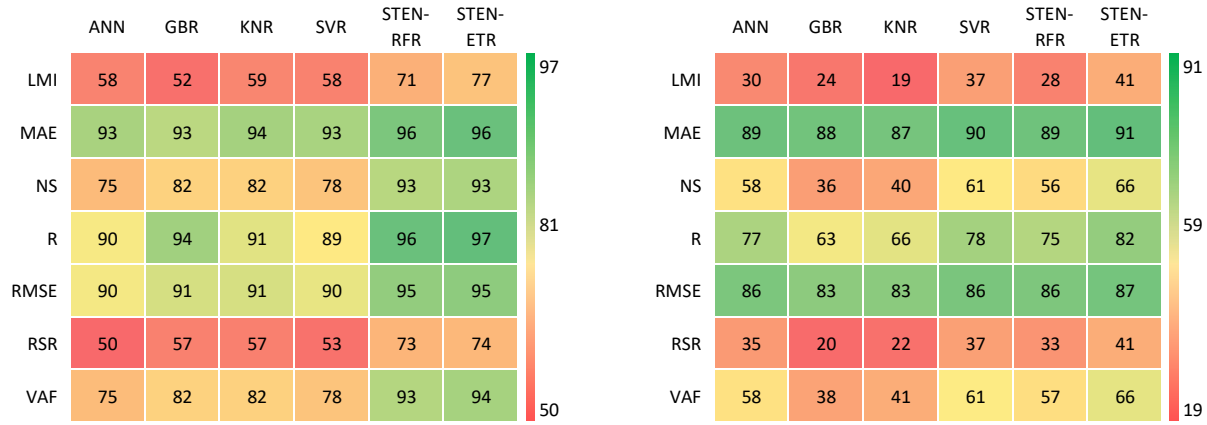

Fig. 7 Accuracy matrix for the testing datasets: (a) for DD and (b) for Fc-28 prediction

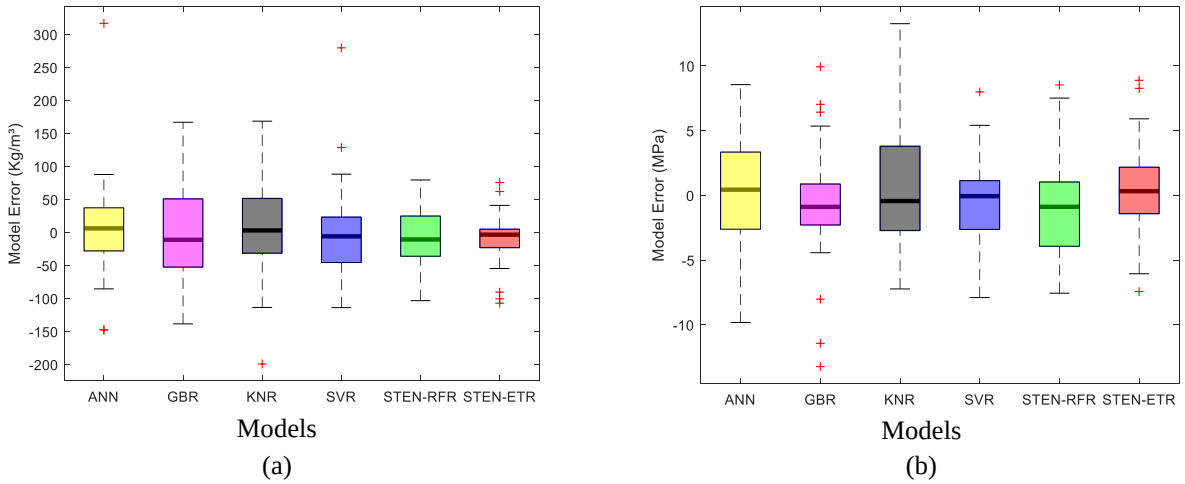

Fig. 8 Boxplot of model's errors for (a) DD and (b) Fc-28

±10% deviation of predicted values with measured values is satisfied for STEN.ETR model in modeling Fc-28, as presented in Fig. 6 for the training and testing stages, respectively. The distortion values around the best fitting in Fig. 6 is high for all models, however, it shown lower with using STEN.ETR model. These results indicates that the STEN.ETR model is the best model among the proposed model in estimating Fc-28 of LWC based on using the whole inputs in the modeling design. Here, it can be concluded that the STEN.ETR model can be considered the best fitting technique can be used to estimate the DD and Fc-28 of LWC. The accuracy of STEN.ETR in estimating the DD and Fc-28 is determined (accuracy=1-(RMSE/(ymax-ymin))). The accuracy of the proposed STEN-ETR model in predicting DD and Fc-28 is found to be 96.79% and 81.50%, respectively.

4.2 Visual interpretation of results

Rather of reading raw reports/results, it is usually preferable to present a visual representation of the collected records in order to find trends, patterns, and other insights. Data visualisation is a technique for presenting raw data in graphical representations that enables viewers to easily explore the data and reveal deep insights. It facilitates rapid and effective comprehension. Taking this into account and analysing the generalization ability of the developed models, visual interpretations of results in terms of accuracy matrix, Taylor diagram and box plot of errors are presented and discussed in this sub-section.

The accuracy matrix is a relatively new type of heat map matrix that enables the estimate of predictive effectiveness based on multiple statistical variables. Fig. 7 shows the accuracy matrices for the DD and Fc-28 prediction models during the testing stage. As can be seen, the proposed STEN-RFR and STEN-ETR are the more accurate models with higher degree of accuracy in all performance matrices.

The boxplot of the proposed models is presented in Fig. 8 to visualize the distribution of model's errors. Here, the de-normalized values are used in boxplot determination. For DD, the interquartile range (IQR), IQR=Q3-Q1, is 65.19, 103.21, 83.10, 68.81, 60.77, and 28.11 Kg/m3 for the ANN, GBR, KNR, SVR, STEN-FRF, and STEN-ETR, respectively. The (zeroth and 100th percentile) of ANN, GBR, KNR, SVR, STEN-FRF, and STEN-ETR are (87.81 and -85.47), (166.94 and -138.45), (168.53 and -113.6), (88.32 and -113.82), (79.52 and -103.30), and (41.0 and 954.60) Kg/m3, respectively. For Fc-28, the IQR is 5.96, 3.16, 6.52, 3.76, 4.96, and 3.59 MPa for the ANN, GBR, KNR, SVR, STEN-FRF, and STEN-ETR, respectively. The

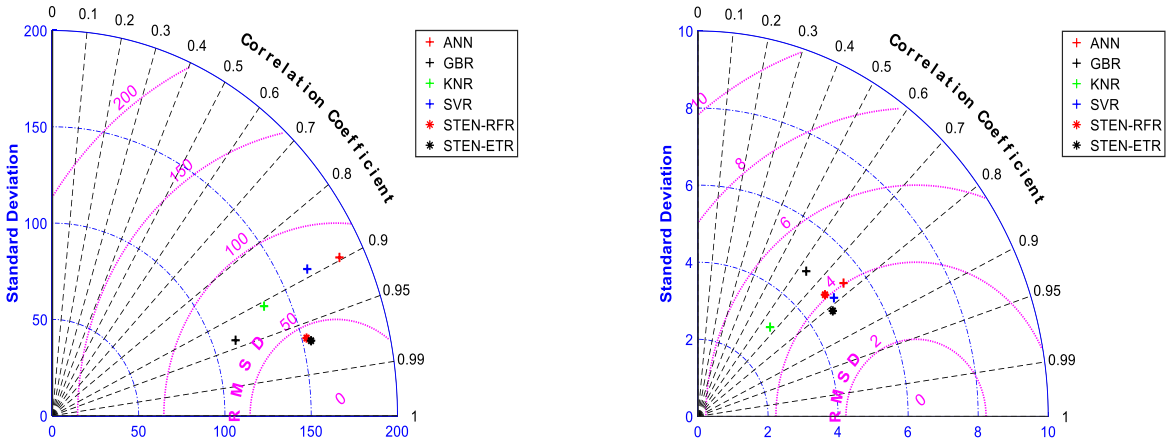

Fig. 9 Taylor diagrams for the testing datasets (a) for DD and (b) for Fc-28 prediction

Table 6 Results of sensitivity analysis (for both DD and Fc-28 prediction)

Variable	DD			FC28		
	Actual	STEN-RFR	STEN-ETR	Actual	STEN-RFR	STEN-ETR
In-1	0.7466	0.7484	0.7495	0.7909	0.7929	0.7960
In-2	0.6851	0.6870	0.6882	0.7323	0.7356	0.7569
In-3	0.4734	0.4777	0.4767	0.5020	0.5247	0.5508
In-4	0.4003	0.4136	0.4104	0.3105	0.3216	0.3253
In-5	0.4418	0.4433	0.4503	0.3343	0.3285	0.3363
In-6	0.4879	0.4882	0.4908	0.3683	0.4048	0.4131
In-7	0.1482	0.0986	0.1191	0.0570	0.0809	0.0797
In-8	0.9492	0.9555	0.9551	0.9411	0.9626	0.9635
In-9	0.6732	0.6906	0.6854	0.6085	0.6432	0.6464
In-10	0.1421	0.1403	0.1397	0.1458	0.1176	0.1299
In-11	0.1018	0.1124	0.0960	0.1440	0.0826	0.0893
In-12	0.0975	0.0997	0.0962	0.1296	0.1289	0.1028
In-13	0.3068	0.2908	0.2957	0.4178	0.3621	0.3814
In-14	0.4547	0.4452	0.4480	0.4686	0.4606	0.4461
In-15	0.5369	0.5517	0.5465	0.5635	0.5706	0.5572
In-16	0.3107	0.3060	0.3109	0.3089	0.3049	0.3257
In-17	0.1635	0.2076	0.1807	0.1694	0.1954	0.1964
In-18	0.1993	0.2070	0.2059	0.2226	0.2468	0.2330
In-19	0.8095	0.8126	0.8133	0.8272	0.8378	0.8482
In-20	0.4957	0.5103	0.5032	0.5454	0.5419	0.5682
In-21	0.8347	0.8395	0.8403	0.8294	0.8489	0.8625

(zeroth and 100th percentile) of ANN, GBR, KNR, SVR, STEN-FRF, and STEN-ETR are (8.55 and -9.82), (5.35 and -4.43), (13.26 and -7.23), (5.40 and -7.89), (7.51 and -7.56), and (5.91 and -6.06) MPa, respectively. These results indicates that the STEN-ETR model is the better to use in modeling DD and Fc-28 of LWC with small variation of model's outliers, as presented in Fig. 8.

The overall evaluation of the proposed models for modelling DD and Fc-28 is presented through Taylor diagram as presented in Fig. 9. The model that has a near distance to zero RMSD can be considered the best model in overall evaluation. From the figure, it can be seen that the developed models STEN-RFR and STEN-ETR outperform other models in modelling DD, while STEN-ETR outperforms other models in estimating Fc-28. Therefore, the developed SREN-ETR model is more robust train and accurate than other models to estimating the DD and Fc-28 of LWC and it can be considered the best hybrid machine

learning for predicting the LWC characteristics.

4.3 Sensitivity analysis

The effect of input variables in modeling DD and Fc-28 of LWC is evaluated through sensitivity analysis. The cosine amplitude method is utilized in this study to determine the input variable impacts. This method is well known in the literature (Kaloop *et al*. 2021, Tanyildizi 2021). In this method, a widely used cosine amplitude method (Kaloop *et al*. 2021) was used to estimate the sensitivity of each input parameter on the outputs, i.e., on DD and Fc-28.

The relationship between inputs and outputs variables is studied using sensitivity analysis. The impact of input variables in modeling DD and Fc-28 of LWC is given in Table 6. The relative impact is presented in between 0 to 1, where 1 represents high impact. Here, the sensitivity of inputs on observed and modeled DD and Fc-28 through SREN-RFR and SREN-ETR is determined. A small variation is detected in impacting all variables in DD and Fc-28 modeling. As shown in Table 6, the high significant variables on DD are aggregate type and content, and for Fc-28, are cement, superplasticizer, and water contents. The aggregate with expanded glass grading 0-1mm and 1mm – 2mm, silica fume, stabilizer, and sand variables impact the DD with medium significant, 0.5~0.8, whereas these variables and aggregate with expanded glass grading 0-1 mm and 2-4 mm impact the Fc-28 of LWC. The impacts of aggregate with expanded clay grading, quartz sand, slag, Nano silica, long fiber variables are seen low, 0.2~0.5, in modeling DD and Fc-28. Finally, eco-glass, limestone powder, fine fly ash, fly ash, and short fiber variables is shown insignificant, lower than 0.2, in modeling DD and Fc-28 of LWC. This means that the significant of cement, water contents, silica fume and aggregate with expanded glass variables is efficient in modeling DD and Fc-28 of LWC.

5. Conclusions

This research aims to use novel hybrid ensemble models in modeling DD and Fc-28 of LWC with density less than 1000 kg/m^3 and to study the impact of concrete constituents' contents for modeling LWC properties. ANN, GBR, KNR, and SVR methods are used, and GBR, KNR, and SVR are integrated with RFR and ETR, STEN-RFR and STEN-ETR, to develop the estimation models. In addition, conventional machine learning is applied to estimate the LWC properties. 140 LWC mixtures were conducted with high variation of 21 input variables are used to model the DD and Fc-28 of LWC and evaluate the sensitivity of each input. The conclusion of finding results can be summarized as follows: The proposed models are efficient to be used in modeling DD of LWC. The conventional machine learning models can be used to estimate the DD. However, the accuracy of hybrid ensemble models is shown better. The model error of STEN.RFR and STEN.ETR is extremely low compared to other models. The RSR is 0.27 and 0.26 for STEN.RFR and STEN.ETR, respectively. The accuracy of both models in terms RMSE is 0.58 Kg/m3 and 0.44 Kg/m3, respectively.

• The SVR and STEN-ETR yield a high correlation with measured Fc-28 values, R=0.78 and =0.82, respectively. In addition, both models ranked high comparing to other proposed models. The IQR is 3.76 and 3.59 MPa for the SVR and STEN-ETR, respectively. GBR and KNR are not significant in modeling Fc-28 of LWC based on the used input variables.

• STEN-ETR model can be considered the best model can be used to estimate the DD and Fc-28 of LWC. The overall evaluation show that efficient in modeling LWC characteristics. While STEN-FRF can be used in modeling DD.

The sensitivity of input variables in modeling DD and Fc-28 of LWC concluded that the fine materials such as limestone powder, fine fly ash, fly ash, and short fibre variables is insignificant in modeling DD and Fc-28 of LWC. Whereas the significant of cement, water contents, silica fume and aggregate with expanded glass variables is shown high in modeling LWC characteristics.

Acknowledgments

This work is supported by the Korea Agency for Infrastructure Technology Advancement (KAIA) grant funded by the Ministry of Land, Infrastructure and Transport (Grant 21CFRP-C163381-01).

References

Abd, A.M. and Abd, S.M. (2017), "Modelling the strength of lightweight foamed concrete using support vector machine (SVM)", *Case Stud. Constr. Mater.*, **6**, 8-15. https://doi.org/10.1016/j.cscm.2016.11.002.

Abdelaziz, N., Abd El-Hakim, R., El-Badawy, S. and Afify, H.A. (2020), "International Roughness Index prediction model for flexible pavements", *Int. J. Pavement Eng.*, **21**(1), 88-99. https://doi.org/10.1080/10298436.2018.1441414.

Abd-Elrahman, M., Chung, S.Y., Sikora, P., Rucinska, T. and Stephan, D. (2019), "Influence of nanosilica on mechanical properties, sorptivity, and microstructure of lightweight concrete", *Materials*, **12**, 3078. https://doi.org/10.3390/ma12193078

Abubakar, A.U. and Tabra, M.S. (2019), "Prediction of compressive strength in high performance concrete with hooked-end steel fiber using K-nearest neighbor algorithm", *Int. J. Integr. Eng.*, **11**(1). https://doi.org/10.30880/ijie.2019.11.01.016.

Alpaydin, E. (2020) *Introduction to Machine Learning*, MIT press.

Alsultan, A. (2021), "Assessment of microstructure and surface effects on vibrational characteristics of public transportation", *Adv. Nano Res.*, **11**(1), 101-113. https://doi.org/10.12989/anr.2021.11.1.101.

Altman, N.S. (1992), "An introduction to kernel and nearest-neighbor nonparametric regression", *Am. Statistician*, **46**(3), 175-185.

Alwash, M.F.A. (2017), "Assessment of concrete strength in existing structures using nondestructive tests and cores : analysis of current methodology and recommendations", Ph.D., Thesis, Université de Bordeaux.

Anyaoha, U., Peng, X. and Liu, Z. (2019), *Concrete Performance*

Prediction Using Boosting Smooth Transition Regression Trees (Boost), in *Nondestructive Characterization and Monitoring of Advanced Materials, Aerospace, Civil Infrastructure, and Transportation XIII*. https://doi.org/10.1117/12.2518279.

Asteris, P.G., Skentou, A., Bardhan, A., Samui, P. and Pilakoutas, K. (2021), "Predicting concrete compressive strength using hybrid ensembling of surrogate machine learning models", *Cem. Concr. Res.*, **145**, 106449. https://doi.org/10.1016/j.cemconres.2021.106449.

Braspenning, P.J., Thuijsman, F. and Weijters, A. (1995) *Artificial Neural Networks: An Introduction to Ann Theory and Practice*, *Psicothema*, Springer Science & Business Media.

Bui, X.N. Jaroonpattanapong, P., Nguyen, H., Tran, Q. and Long, N. (2019), "A novel hybrid model for predicting blast-induced ground vibration based on k-nearest neighbors and particle swarm optimization", *Sci. Rep.*, **9**(1), 1-14. https://doi.org/10.1038/s41598-019-50262-5.

Chakraborty, D., Awolusi, I. and Gutierrez, L. (2021), "An explainable machine learning model to predict and elucidate the compressive behavior of high-performance concrete", *Results Eng.*, **11**, 100245. https://doi.org/10.1016/j.rineng.2021.100245.

Chou, J.S., Ngo, N.T. and Pham, A.D. (2016), "Shear strength prediction in reinforced concrete deep beams using nature-inspired metaheuristic support vector regression", *J. Comput. Civ. Eng.*, **30**(1), 04015002. https://doi.org/10.1061/(asce)cp.1943-5487.0000466.

Chung, S.Y., Abd Elrahman, M., Kim, JS., Han, TS., Stephan, D. and Sikora, P. (2019), "Comparison of lightweight aggregate and foamed concrete with the same density level using image-based characterizations", *Constr. Build. Mater.*, **211**, 988-999. https://doi.org/10.1016/j.conbuildmat.2019.03.270.

Cui, L., Chen, P., Wang, L., Li, J. and Ling, H. (2021), "Application of extreme gradient boosting based on grey relation analysis for prediction of compressive strength of concrete", *Adv. Civ. Eng.*, 8878396. https://doi.org/10.1155/2021/8878396.

Du, H., Du, S. and Liu, X. (2015), "Effect of nano-silica on the mechanical and transport properties of lightweight concrete", *Constr. Build. Mater.*, **82**, 114-122.

Fatahi, O. and Jafari, S. (2018), "Prediction of lightweight aggregate concrete compressive strength", *J. Rehabil. Civ. Eng.*, **6**(2), 154-163. https://doi.org/10.22075/jrce.2017.11556.1192.

Friedman, J.H. (2001), "Greedy function approximation: A gradient boosting machine", *Ann. Stat.*, **29**(5), 1189-1232. https://doi.org/10.1214/aos/1013203451.

Gabr, A.R., Roy, B., Kaloop, M.R., Kumar, D., Arisha, A., Shiha, M., Shwally, S., Hu, J. and El-Badawy, S. (2021), "A novel approach for resilient modulus prediction using extreme learning machine-equilibrium optimiser techniques", *Int. J. Pavement Eng.*, 1-11. https://doi.org/10.1080/10298436.2021.1892109.

Geurts, P., Ernst, D. and Wehenkel, L. (2006), "Extremely randomized trees", *Mach. Learn.*, **63**(1), 3-42. https://doi.org/10.1007/s10994-006-6226-1.

Gouasmi, M.T., Benosman, A.S., Taïbi, H., Kazi-Tani, N. and Belbachir, M. (2017), "Destructive and non-destructive testing of an industrial screed mortar made with lightweight composite aggregates WPLA", *Int. J. Eng. Res. Africa*, **33**, 140-158. https://doi.org/10.4028/www.scientific.net/JERA.33.140.

Hadianfard, M.A. and Jafari, S. (2016), "Prediction of lightweight aggregate concrete compressive strength using ultrasonic pulse velocity test through gene expression programming", *Sci. Iran.*, **23**(6), 2506-2513. https://doi.org/10.24200/sci.2016.2309.

Jalal, F.E., Xu, Y., Iqbal, M., Jamhiri, B. and Javed, M. (2021), "Predicting the compaction characteristics of expansive soils using two genetic programming-based algorithms", *Transp. Geotech.*, **30**, 100608. https://doi.org/10.1016/j.trgeo.2021.100608.

Kaloop, M.R., El-Badawy, S.M., Ahn, J., Sim, H., Hu, J. and Abd El-Hakim, R. (2020), "A hybrid wavelet-optimally-pruned extreme learning machine model for the estimation of international roughness index of rigid pavements", *Int. J. Pavement Eng.*, 1-15. https://doi.org/10.1080/10298436.2020.1776281.

Kaloop, M.R., Samui, P., Shafeek, M. and Hu, J. (2020), "Estimating slump flow and compressive strength of self-compacting concrete using emotional neural networks", *Appl. Sci.*, **10**(23), 8543. https://doi.org/10.3390/app10238543.

Kaloop, M.R., Bardhan, A., Kardani, N., Samui, P., Hu, J. and Ramzy, A. (2021), "Novel application of adaptive swarm intelligence techniques coupled with adaptive network-based fuzzy inference system in predicting photovoltaic power", *Renew. Sustain. Energy Rev.*, **148**, 111315. https://doi.org/10.1016/j.rser.2021.111315.

Kaloop, M.R., Elrahman, M.A. and Hu, J.W. (2022), "Nondestructive tests for defections detection of nanoparticles in cement-based materials: A review", *Adv. Nano Res.*, **12**(1), 1-23. https://doi.org/10.12989/anr.2022.12.1.001.

Kasiri, R. and Massah, S. (2022), "Mathematical modeling of concrete beams containing GO nanoparticles for vibration analysis and measuring their compressive strength using an experimental method", *Adv. Nano Res.*, **12**(1), 73-79, https://doi.org/10.12989/anr.2022.12.1.073

Khan, M.U.A., Shukla, S.K. and Raja, M.N.A. (2021), "Soil-conduit interaction: an artificial intelligence application for reinforced concrete and corrugated steel conduits", *Neural Comput. Appl.*, **33**(21), 14861-14885. https://doi.org/10.1007/s00521-021-06125-0.

Khater, H.M. (2016), "Nano-Silica effect on the physicomechanical properties of geopolymer composites", *Adv. Nano Res.*, **4**(3), 181-195, https://doi.org/10.12989/anr.2016.4.3.181

Koya, B.P., Aneja, S., Gupta, R. and Valeo, C. (2021), "Comparative analysis of different machine learning algorithms to predict mechanical properties of concrete", *Mech. Adv. Mater. Struct.* 1-18. https://doi.org/10.1080/15376494.2021.1917021.

Lee, D.G. and Ahn, K.H. (2021), "A stacking ensemble model for hydrological post-processing to improve streamflow forecasts at medium-range timescales over South Korea", *J. Hydrol.*, **600**, 126681. https://doi.org/10.1016/j.jhydrol.2021.126681.

Lin, C.J. and Wu, N.J. (2021), "An ANN model for predicting the compressive strength of concrete", *Appl. Sci.*, **11**(9), 3798. https://doi.org/10.3390/app11093798.

Marani, A. and Nehdi, M.L. (2020), "Machine learning prediction of compressive strength for phase change materials integrated cementitious composites", *Constr. Build. Mater.*, **265**, 120286. https://doi.org/10.1016/j.conbuildmat.2020.120286.

Meshram, S.G., Singh, V., Kisi, O., Karimi, V. and Meshram, C. (2020), "Application of artificial neural networks, support vector machine and multiple model-ANN to sediment yield prediction", *Water Resour. Manag.*, **34**(15), 4561-4575. https://doi.org/10.1007/s11269-020-02672-8.

Mozumder, R.A., Roy, B. and Laskar, A.I. (2017), "Support vector regression approach to predict the strength of FRP confined concrete", *Arab. J. Sci. Eng.*, **42**(3), 1129-1146. https://doi.org/10.1007/s13369-016-2340-y.

Nagarajan, D., Rajagopal, T. and Meyappan, N. (2020), "A comparative study on prediction models for strength properties of LWA concrete using artificial neural network", *Rev. Constr.*, 103-111. https://doi.org/10.7764/rdlc.19.1.103-111.

Naniz, O.A. and Mazloom, M. (2018), "Effects of colloidal nano-silica on fresh and hardened properties of self-compacting lightweight concrete", *J. Build. Eng.*, **20**, 400-410.

Narasimman, K., Jassam, T., Velayutham, T.S., Yaseer, M. and Ruzaima, R. (2020), "The synergic influence of carbon nanotube and nanosilica on the compressive strength of lightweight concrete", *J. Build. Eng.*, **32**, 101719.

Nguyen-Sy, T., Wakim, J., To, Q., Vu, M., Nguyen, T. and Nguyen, T.T. (2020), "Predicting the compressive strength of concrete from its compositions and age using the extreme gradient boosting method", *Constr. Build. Mater.*, **260**, 119757. https://doi.org/10.1016/j.conbuildmat.2020.119757.

Nie, P., Roccotelli, M., Fanti, M., Ming, Z. and Li, Z. (2021), "Prediction of home energy consumption based on gradient boosting regression tree", **7**, 1246-1255. https://doi.org/https://doi.org/10.1016/j.egyr.2021.02.006.

Pal, M. and Deswal, S. (2011), "Support vector regression based shear strength modelling of deep beams", *Comput. Struct.*, **89**(13), 1430-1439. https://doi.org/10.1016/j.compstruc.2011.03.005.

Sandhu, A.K. and Batth, R.S. (2021), "Software reuse analytics using integrated random forest and gradient boosting machine learning algorithm", *Softw. Pract. Exp.*, **51**(4), 735-747. https://doi.org/10.1002/spe.2921.

Sedghi, Y., Zandi, Y., Paknahad, M., Assilzadeh, H. and Khadimallah, M. (2021), "Optimization of shear connectors with high strength nano concrete using soft computing techniques", *Adv. Nano Res.*, **11**(6), 595-606. https://doi.org/10.12989/anr.2021.11.6.595.

Shariati, A., Barati, M., Ebrahimi, F. and Toghroli, A. (2020), "Investigation of microstructure and surface effects on vibrational characteristics of nanobeams based on nonlocal couple stress theory", *Adv. Nano Res.*, **8**(3), 191-202. https://doi.org/10.12989/anr.2021.11.6.595.

Sidiq, S.J., Zaman, M. and Butt, M. (2018), "An empirical comparison of classifiers for multi-class imbalance learningNo Title", *Int. J. Data Min. Emerg. Technol.*, **8**(1), 115-122.

Sikora, P., Rucinska, T., Stephan, D., Chung, S. and Abd Elrahman, M. (2020), "Evaluating the effects of nanosilica on the material properties of lightweight and ultra-lightweight concrete using image-based approaches", *Constr. Build. Mater.*, **264**, 120241. https://doi.org/10.1016/j.conbuildmat.2020.120241.

Tanyildizi, H. (2021), "Predicting the geopolymerization process of fly ash-based geopolymer using deep long short-term memory and machine learning", *Cem. Concr. Compos.*, **123**, 104177. https://doi.org/10.1016/j.cemconcomp.2021.104177.

Tavakkol, S., Alapour, F., Kazemian, A., Hasaninejad, A., Ghanbari, A. and Ramezanianpour, A.A. (2013), "Prediction of lightweight concrete strength by categorized regression, MLR and ANN", *Comput. Concr.*, **12**(2), 151-167. https://doi.org/10.12989/cac.2013.12.2.151.

Tuhta, S. (2021), "The determination of effect of TiO2 on dynamic behavior of scaled concrete structure by OMA", *Adv. Nano Res.*, **11**(6), 641-648. https://doi.org/10.12989/anr.2021.11.6.641

Vapnik, V. (1995) *The Nature of Statistical Learning Theory*. Springer, New York, U.S.A.

Wan, Z., Xu, Y. and Šavija, B. (2021), "On the use of machine learning models for prediction of compressive strength of concrete: Influence of dimensionality reduction on the model performance", *Materials*, **14**(4), 713. https://doi.org/10.3390/ma14040713.

Wong, L.S., Marani, A. and Nehdi, M.L. (2021), "Gradient boosting coupled with oversampling model for prediction of concrete pipe-joint infiltration using designwise data set", *J. Pipeline Syst. Eng. Pract.*, **12**(3), 04021015. https://doi.org/10.1061/(asce)ps.1949-1204.0000557.

Wu, N.J. (2021), "Predicting the compressive strength of concrete using an RBF-ANN model", *Appl. Sci.*, **11**(14), 6382. https://doi.org/10.3390/app11146382.

Yaseen, Z.M., Tran, M., Kim, S., Bakhshpoori, T. and Deo, R. (2018), "Shear strength prediction of steel fiber reinforced concrete beam using hybrid intelligence models: A new approach", *Eng. Struct.*, **177**, 244-255. https://doi.org/10.1016/j.engstruct.2018.09.074.

Yoon, J.Y., Kim, H., Lee, Y. and Sim, S. (2019), "Prediction model for mechanical properties of lightweight aggregate concrete using artificial neural network", *Materials*, **12**(17), 2678. https://doi.org/10.3390/ma12172678.

Zanoni, M., Arcelli Fontana, F. and Stella, F. (2015), "On applying machine learning techniques for design pattern detection", *J. Syst. Softw.*, **103**, 102-117. https://doi.org/https://doi.org/10.1016/j.jss.2015.01.037.

Zhou, C., Zhou, L., Liu, F., Chen, W., Wang, Q., Liang, K., Guo, W. and Zhou, L. (2021), "A novel stacking heterogeneous ensemble model with hybrid wrapper-based feature selection for reservoir productivity predictions", *Complexity*, 6675638. https://doi.org/10.1155/2021/6675638.

SR